Asynchronous optical sampling with arbitrary detuning between laser repetition rates

Laura Antonucci, Xavier Solinas, Adeline Bonvalet, Manuel Joffre

Asynchronous optical sampling with arbitrary detuning between laser repetition rates

Laura Antonucci,[1,2] **Xavier Solinas,**[1,2] **Adeline Bonvalet,**[1,2] **and Manuel Joffre**[1,2,*]

[1]*Laboratoire d'Optique et Biosciences, Ecole Polytechnique, Centre National de la Recherche Scientifique, 91128 Palaiseau, France*
[2]*Institut National de la Santé et de la Recherche Médicale, U696, 91128 Palaiseau, France*
[*]*manuel.joffre@polytechnique.edu*

Abstract: A method of asynchronous optical sampling based on free-running lasers with no requirement on the repetition rates is presented. The method is based on the *a posteriori* determination of the delay between each pair of pulses. A resolution better than 400 fs over 13 ns total delay scan is demonstrated. In addition to the advantages of conventional asynchronous sampling techniques, this method allows a straightforward implementation on already-existing laser systems using a fiber-based setup and an appropriate acquisition procedure.

OCIS codes: (320.7100) Ultrafast measurements; (320.7160) Ultrafast technology.

References and links

1. G. Sucha, M. E. Fermann, D. J. Harter, and M. Hofer, "A new method for rapid temporal scanning of ultrafast lasers," IEEE J. Sel. Top. Quantum Electr. **2,** 605–621 (1996).
2. M. A. Duguay and J. W. Hansen, "Optical sampling of subnanosecond light pulses," Appl. Phys. Lett. **13,** 178–180 (1968).
3. E. Lill, S. Schneider, and F. Dorr, "Rapid optical sampling of relaxation-phenomena employing 2 time-correlated picosecond pulsetrains," Appl. Phys. **14,** 399–401 (1977).
4. P. A. Elzinga, R. J. Kneisler, F. E. Lytle, Y. Jiang, G. B. King, and N. M. Laurendeau, "Pump probe method for fast analysis of visible spectral signatures utilizing asynchronous optical-sampling," Appl. Opt. **26,** 4303–4309 (1987).
5. P. A. Elzinga, F. E. Lytle, Y. Jian, G. B. King, and N. M. Laurendeau, "Pump probe spectroscopy by asynchronous optical-sampling," Appl. Spectrosc. **41,** 2–4 (1987).
6. J. D. Kafka, J. W. Pieterse, and M. L. Watts, "2-color subpicosecond optical-sampling technique," Opt. Lett. **17,** 1286–1288 (1992).
7. F. Keilmann, C. Gohle, and R. Holzwarth, "Time-domain mid-infrared frequency-comb spectrometer," Opt. Lett. **29,** 1542–1544 (2004).
8. D. S. Kim, J. Y. Sohn, J. S. Yahng, Y. H. Ahn, K. J. Yee, D. S. Yee, Y. D. Jho, S. C. Hohng, D. H. Kim, W. S. Kim, J. C. Woo, T. Meier, S. W. Koch, D. H. Woo, E. K. Kim, and S. H. Kim, "Femtosecond four-wave mixing experiments on GaAs quantum wells using two independently tunable lasers," Phys. Rev. Lett. **80,** 4803–4806 (1998).
9. Y. Takagi and S. Adachi, "Subpicosecond optical sampling spectrometer using asynchronous tunable mode-locked lasers," Rev. Sci. Instr. **70,** 2218–2224 (1999).
10. A. Bartels, F. Hudert, C. Janke, T. Dekorsy, and K. Kohler, "Femtosecond time-resolved optical pump-probe spectroscopy at kilohertz-scan-rates over nanosecond-time-delays without mechanical delay line," Appl. Phys. Lett. **88,** 041117 (2006).
11. F. Hudert, A. Bruchhausen, D. Issenmann, O. Schecker, R. Waitz, A. Erbe, E. Scheer, T. Dekorsy, A. Mlayah, and J. R. Huntzinger, "Confined longitudinal acoustic phonon modes in free-standing Si membranes coherently excited by femtosecond laser pulses," Phys. Rev. B **79,** 201307 (2009).

---

12. R. Gebs, G. Klatt, C. Janke, T. Dekorsy, and A. Bartels, "High-speed asynchronous optical sampling with sub-50fs time resolution," Opt. Express **18,** 5974–5983 (2010).
13. A. Schliesser, M. Brehm, F. Keilmann, and D. W. van der Weide, "Frequency-comb infrared spectrometer for rapid, remote chemical sensing," Opt. Express **13,** 9029–9038 (2005).
14. T. Yasui, E. Saneyoshi, and T. Araki, "Asynchronous optical sampling terahertz time-domain spectroscopy for ultrahigh spectral resolution and rapid data acquisition," Appl. Phys. Lett. **87,** 061101 (2005).
15. C. Janke, M. Forst, M. Nagel, H. Kurz, and A. Bartels, "Asynchronous optical sampling for high-speed characterization of integrated resonant terahertz sensors," Opt. Lett. **30,** 1405–1407 (2005).
16. T. Yasui, Y. Kabetani, E. Saneyoshi, S. Yokoyama, and T. Araki, "Terahertz frequency comb by multifrequency-heterodyning photoconductive detection for high-accuracy, high-resolution terahertz spectroscopy," Appl. Phys. Lett. **88,** 241104 (2006).
17. A. Bartels, A. Thoma, C. Janke, T. Dekorsy, A. Dreyhaupt, S. Winnerl, and M. Helm, "High-resolution THz spectrometer with kHz scan rates," Opt. Express **14,** 430–437 (2006).
18. S. Schiller, "Spectrometry with frequency combs," Opt. Lett. **27,** 766–768 (2002).
19. C. Dorrer, D. C. Kilper, H. R. Stuart, G. Raybon, and M. G. Raymer, "Linear optical sampling," IEEE Phot. Techn. Lett. **15,** 1746–1748 (2003).
20. I. Coddington, W. C. Swann, and N. R. Newbury, "Coherent multiheterodyne spectroscopy using stabilized optical frequency combs," Phys. Rev. Lett. **100,** 013902 (2008).
21. S. Kray, F. Spoler, M. Forst, and H. Kurz, "Dual femtosecond laser multiheterodyne optical coherence tomography," Opt. Lett. **33,** 2092–2094 (2008).
22. J. D. Deschenes, P. Giaccari, and J. Genest, "Optical referencing technique with CW lasers as intermediate oscillators for continuous full delay range frequency comb interferometry," Opt. Express **18,** 23358–23370 (2010).
23. I. Coddington, W. C. Swann, and N. R. Newbury, "Time-domain spectroscopy of molecular free-induction decay in the infrared," Opt. Lett. **35,** 1395–1397 (2010).
24. B. Bernhardt, A. Ozawa, P. Jacquet, M. Jacquey, Y. Kobayashi, T. Udem, R. Holzwarth, G. Guelachvili, T. W. Hansch, and N. Picque, "Cavity-enhanced dual-comb spectroscopy," Nat. Photonics **4,** 55–57 (2010).
25. J. Bredenbeck, J. Helbing, and P. Hamm, "Continuous scanning from picoseconds to microseconds in time resolved linear and nonlinear spectroscopy," Rev. Sci. Instr. **75,** 4462-4466 (2004).
26. A. C. Yu, X. Ye, D. Ionascu, W. X. Cao, and P. M. Champion, "Two-color pump-probe laser spectroscopy instrument with picosecond time-resolved electronic delay and extended scan range," Rev. Sci. Instr. **76,** 114301 (2005).
27. J. Davila-rodriguez, M. Bagnell, C. Williams, and P. J. Delfyett, "Multiheterodyne detection for spectral compression and downconversion of arbitrary periodic optical signals," J. Lightwave Technol. **29,** 3091–3098 (2011).
28. L. Noirie, F. Cérou, G. Moustakides, O. Audouin, and P. Peloso, "New transparent optical monitoring of the eye and ber using asynchronous under-sampling of the signal," Proc. Eur. Conf. Optical Communication, PD2.2 (2002).
29. M. Westlund, H. Sunnerud, M. Karlsson, and P. A. Andrekson, "Software-synchronized all-optical sampling for fiber communication systems," J. Lightwave Technol. **23,** 1088–1099 (2005).
30. T. Mori and A. Otani, "A Simple Synchronization Method for Optical Sampling Eye Monitor," Jpn. J. Appl. Phys. **49,** 070208 (2010).
31. K. Dou, A. Débarre, J.-L. Le Gouët, I. Lorgeré, and P. Tchénio, "Field cross correlator for analysis of ultrafast signals," Appl. Opt. **33,** 7980–7986 (1994).

1. Introduction

Many applications of femtosecond lasers, such as time-resolved pump-probe spectroscopy, rely on pairs of ultrashort pulses with a well known and variable time delay used to explore the temporal dynamics of the sample under study. In most cases, the pulse pair is generated by splitting a femtosecond laser beam into two arms that are recombined after a variable optical path is applied to one of the two arms by use of a translation stage. Although this method is well suited for short time delays, it does suffer from several drawbacks that have been discussed previously [1]. In particular, for time delays longer than 1 ns, corresponding to an added optical path of more than 30 cm, issues such as defocusing, misalignment and scanning speed must be considered.

To overcome these difficulties, methods based on two different laser systems synchronized by electronic means have been developed, allowing much greater values of the accessible time delay and the ability for extremely fast scanning over the time range of interest. The most widely used approach is asynchronous optical sampling (ASOPS), a stroboscopic method based on the

use of two femtosecond oscillators that allows extremely fast scanning on a broad time range extending up to the laser period [1–7]. This method has found numerous applications, e.g. in pump-probe or four-wave mixing spectroscopy [5,8–12], and Fourier-transform spectroscopy in the mid-infrared [7,13] and far-infrared (or THz) [14–17]. In association with frequency-comb technologies, this approach - also termed multi-heterodyne coherent spectroscopy - allows to reach the near infrared and visible spectral domains, and is in the process of revolutionizing Fourier-transform spectroscopy [7, 18–24].

Another example of electronic control of the time delay is the use of two femtosecond amplifiers seeded by phase-locked oscillators running at identical repetition rates. Coarse control of the time delay is then achieved through the trigger signals firing the two amplifiers, whereas fine tuning is achieved by phase shifting the two oscillators [25, 26]. This results in a complete electronic control of the time delay with virtually no upper limit in the accessible time range, since such lasers can be fired even in single-shot mode.

All methods described above require the use of two femtosecond oscillators with repetition rates that are either identical or almost identical, or in some cases near multiples [2, 27]. This condition must be taken into account at an early stage of the experiment design, as it requires the use of dedicated oscillators specially set up for this purpose. In this letter, we demonstrate an ASOPS variant that does not have such a limitation and can be applied to any couple of femtosecond oscillators, with arbitrary detuning between their repetition rates. This new method, coined AD-ASOPS for arbitrary detuning ASOPS, should help the straightforward application of asynchronous sampling to pre-existing setups, thereby greatly extending opportunities for new experiments. We note that our approach is closely related to an optical sampling method developed in the field of optical telecommunications for the specific purpose of characterizing eye diagrams or bit error rates, in which case a software synchronization method can rely on the signal itself for *a posteriori* recovery of the time axis [28–30].

2. Principle of operation

Let us consider two femtosecond oscillators of repetition rates f_1 and f_2. We call $T_1 = 1/f_1$ and $T_2 = 1/f_2$ the corresponding periods of the pulse trains. In the following, we will assume that the first laser is used to produce the pump pulses, whereas the second laser, of frequency f_2, will be used as the probe.
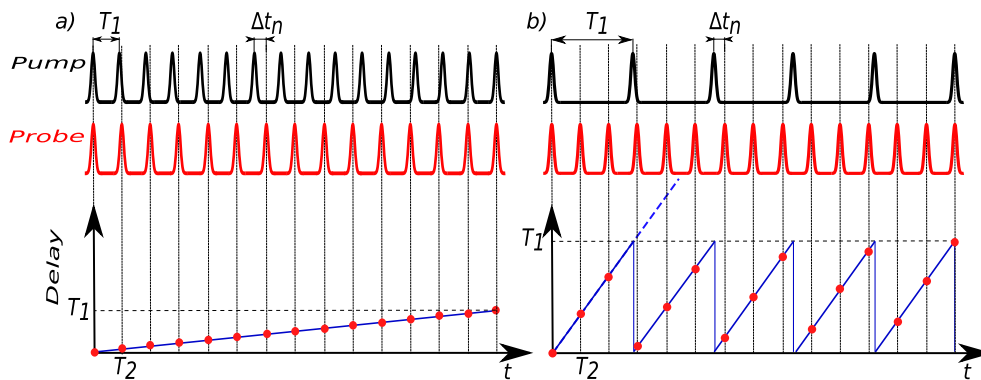

Fig. 1. (a) Principle of conventional ASOPS, which relies on two femtosecond oscillators with almost identical repetition rates, resulting in a slow linear increment of the pump-probe time delay. (b) In AD-ASOPS the delay varies much more rapidly with time but still takes well defined values that can be accurately determined as described in the text.

In conventional ASOPS, $f_1 \sim f_2$, so that there is a slow linear increment of the time delay between the pump and probe pulses, as shown in Fig. 1(a). Let us assume that the two pulse trains are initially in coincidence. Until the next coincidence occurs, the pump-probe time delay associated with subsequent pulse pairs then obeys the simple law

$$\Delta t_n = n(T_2 - T_1) \tag{1}$$

where n is the probe pulse number, starting with $n = 0$ on coincidence. The sampling interval is thus equal to $|T_2 - T_1| = \Delta f / (f_1 f_2)$, where $\Delta f = |f_2 - f_1|$ is the detuning between the repetition rates of the two oscillators. Note that Δf is also the scanning rate, as the next coincidence will occur after a time $1/\Delta f$. Since in ASOPS the sampling interval governs the time resolution, the scanning rate is usually chosen to be a small fraction of the laser repetition rate, typically in the Hz or kHz range.

In AD-ASOPS, f_1 and f_2 take arbitrary values, so that the detuning Δf can be of the order of tens of MHz, resulting in a much more rapid variation of the time delay. However, the linear dependence still holds, though with a much greater slope, as shown with the blue dashed line in Fig. 1(b). The time delay thus obeys a law similar to that of eq. 1, except that the actual delay - which cannot be greater than the period of the pump laser - must be wrapped inside the interval $[0, T_1[$ by using the above value modulo T_1:

$$\Delta t_n = n(T_2 - T_1) [T_1] = nT_2 [T_1] \tag{2}$$

where $[T_1]$ stands for modulo T_1. In practice, the acquisition system will simply detect coincidences and count the number of pulses delivered by each laser between coincidence events, termed respectively N_1 and N_2. Replacing T_2 with $T_1 \times N_1/N_2$ in eq. 2 yields the actual time delay for the acquisition associated with pulse number n between the two coincidence events:

$$\Delta t_n = \left\{ n \frac{N1}{N2} \right\} T_1 \tag{3}$$

where $\{x\}$ stands for the fractional part of x. By dividing the time axis in time bins of width set by the user in order to insure proper signal sampling, the probe signal measured for pulse number n is then sorted in the appropriate time bin according to the calculated time delay Δt_n, for $0 \leq n \leq N_2$. The whole process is repeated for each pair of coincidence events. Although time slots are filled in an apparently quasi-random fashion, instead of the usual sequential filling, a complete scan can be obtained after appropriate data averaging. As in ASOPS, the time accuracy of AD-ASOPS will be ultimately limited by the uncertainty in measuring coincidences and in deviation in the linear variation of the delay due to laser jitter.

3. Coincidence detection

In previous work on ASOPS, coincidences between the two lasers have been detected using a nonlinear interaction, such as sum-frequency mixing [6, 9, 15]. Although such a method is more general and could easily be combined with AD-ASOPS, the pump and probe lasers used in our experiment turn out to have overlapping spectra so we chose to use a linear method instead, consisting of measuring the interference between individual collinearly-recombined laser pulses. Indeed, if the pulses do not overlap in time, the total measured power will be simply equal to the sum of the two laser powers. In contrast, if the two pulses overlap in time, the coherent interaction between individual pump and probe pulses will most often result in a constructive or destructive interference. The corresponding measured signal will thus be either greater or smaller than the reference value, triggering a coincidence detection whenever the deviation is greater than a specified threshold.
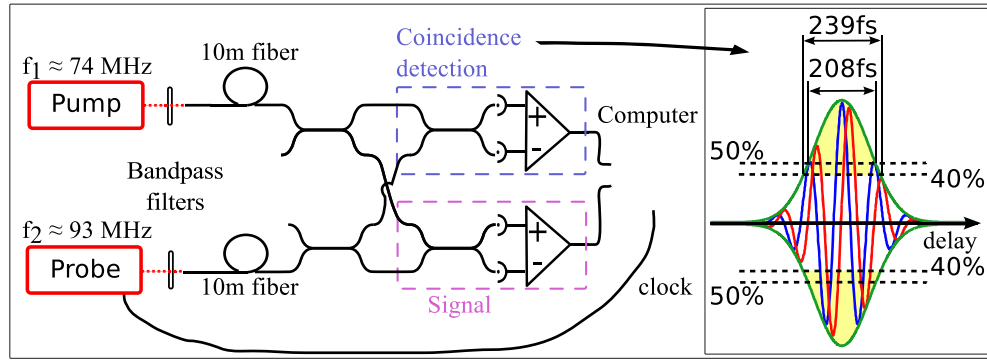
Fig. 2. Experimental setup used to demonstrate AD-ASOPS. The insert shows the interference signal used for coincidence detection: the blue and red curves are examples of signals associated with two different carrier envelope phases; the green line is the envelope of all possible signals; the yellow area indicates the signals inducing coincidence detection.

The experimental setup is shown in Fig. 2. The asynchronous scanning is performed with two Ti:Sapphire femtosecond lasers oscillating at 74 MHz (Femtolasers, Synergy PRO) and 93 MHz (home-made) with spectral full width at half maximum (FWHM) of 100 nm and 50 nm respectively and centered at 800 nm. A more precise value of the two repetition rates is measured before each measurement run using a frequency-meter. Since the two lasers are placed in two different experimental rooms, it is convenient to bring a small energy percentage of their beams in vicinity by use of two 10-m long, single-mode optical fibers. On each beam, a fiber-optic coupler (Thorlabs, FC850-40-50-APC) allows to split the pulses so as to direct them towards the coincidence-detection (blue dashed line) and signal (magenta dashed line) parts of the setup. For coincidence detection, another fiber optic coupler recombines the pump and probe pulses and the resulting interference signal, depicted in the figure insert, is directly detected by use of a balanced detector (Thorlabs, PDB130A-AC). The analog signal is then converted to digital data with a 210 MS/s, 14-bit analog to digital acquisition card (Innovative, X5-210M), clocked at frequency f_2 by a signal generated from the probe laser.

Obviously, some coincidence events will remain undetected by this setup whenever the two pulses are nearly in quadrature, which may randomly occur depending on the carrier-envelope phases (CEP) and on the fast oscillation of the interference signal with respect to time delay. Although this effect could be taken care of by use of a dual-quadrature interferometer [19, 31], we preferred to use the simpler setup presented here and tolerate a slight decrease of the rate of detected coincidences. We note that a threshold set at 40% of the maximum signal allows the detection of roughly 70% of all coincidence events. The advantage of using a linear method for coincidence detection is that the ultimate accuracy is not limited by the final pulse duration (stretched to more than 10 ps after propagation through a 10-m long fiber). Indeed, the linear interference signal depends on the difference between the spectral phases of the two pulses, which compensates thanks to the matching in fiber length. The associated coherence time can be calculated from the product of the spectral intensities of the two pulses, evaluated from the experimentally-measured spectra to be 3.0 THz FWHM. This value is much smaller than the initial spectral widths of the two lasers due to the fact that two bandpass filters are placed just before the entrance of the optical fiber in order to match the two spectra and enhance the contrast of the interference signal. Assuming a gaussian profile, the resulting spectral width yields a coherence time of 208 fs FWHM, or a coincidence detection window Δt_c of 239 fs taking into account the 40% threshold value. Note that this finite time resolution is responsible for the fact

that the ratio f_1/f_2, which is an arbitrary real number, can be approximated with the rational number N_1/N_2 introduced in section 2. Hence, there is no additional uncertainty associated with the fact that N_1 and N_2 are integer numbers apart from the minimal time resolution of Δt_c.

A rough estimate of the coincidence rate can be obtained by assuming that coincidences are random events with a probability equal to the ratio between the coincidence detection window $\Delta t_c \approx 240$ fs and the pump period $T_1 \approx 13.5$ ns. This yields a probability of about 1.8×10^{-5}. Multiplying by the probe laser repetition rate yields a coincidence rate $f_1 f_2 \Delta t_c$ of about 1.6 kHz, which drops to 1.15 kHz when taking into account that only 70% of all coincidences are detected by our experimental scheme, as discussed above. This corresponds to an average time between coincidences slightly smaller than 900 μs. In practice, we have measured an average coincidence rate of 1.06 kHz, in excellent agreement with the above estimate. However, this is only an average value and, in contrast with conventional ASOPS, there is a broad distribution of possible time delays between two coincidences. The associated probability density function is shown in Fig. 3 and exhibits an exponential decay (time constant roughly 800 μs) for large values of the delay. This rather rapid decay insures that the detrimental effect of laser jitter – more important for larger delays – remains limited.
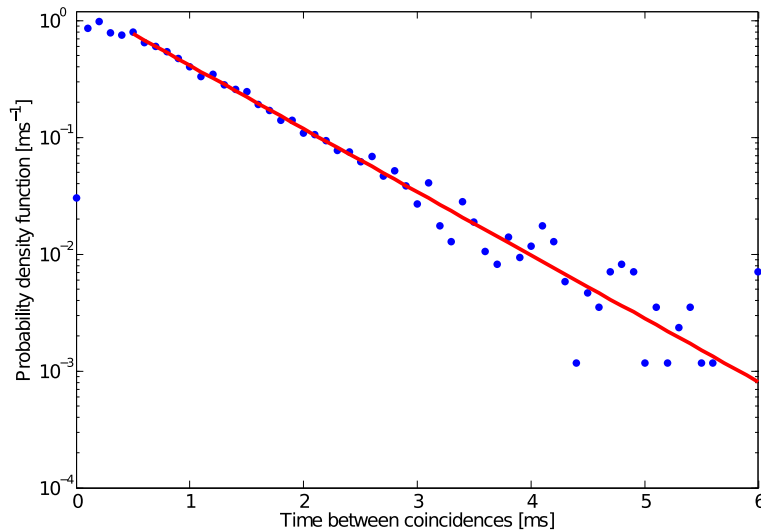

Fig. 3. Semi-logarithmic plot of the measured probability density function of coincidence events as a function of the time elapsed between two coincidences (blue dots). The data have been obtained by computing the histogram of coincidence events according to the times elapsed from the previous coincidence sorted in time bins of 100 μs. The data corresponding to an elapsed time greater than 500 μs have been fitted to an exponentially decaying function (red solid line), with a time constant of 802 μs.

4. Experimental results

In order to characterize the accuracy of the method, we used an interferometer, shown in the magenta-outlined area in Fig. 2, similar to that described above for coincidence detection. However, instead of the binary signal generated for coincidence detection, we use here the complete analog signal produced by the balanced detector. In order to avoid averaging out constructive and destructive interferences, we accumulate the square of the signal deviation - or variance. For all samples corresponding to a specific time bin, the measured signal is thus the average over all selected data points of the signal square minus the square of the average signal. In prac-

tice, the acquisition card provides a continuous flow of data packets processed by a C-language program which calculates the time delay for each probe pulse, using an interpolation between the previous and next coincidences by use of eq. 3, and the associated signal is then averaged in the corresponding time bin. Performing both acquisition and processing in a mid-range personal computer hosting a quad-core processor (Xeon, Intel) running at 2.33 GHz, we achieved a maximum processing rate of about 37×10^6 samples/second, which is only 40% of the probe laser repetition rate. We thus had to skip 60% of the acquired data packets in order to keep track with the acquisition flow. This has no effect on the averaged data and merely halves the actual acquisition rate. We expect that ongoing progress in computing power or enhanced parallelization, e.g. in graphics processing units, would allow to process the data at hundreds of MHz in mid-range personal computers. Furthermore, a dedicated hardware based on a Field-Programmable Gate Array (FPGA) would easily achieve the required processing rate for data processing in real time.
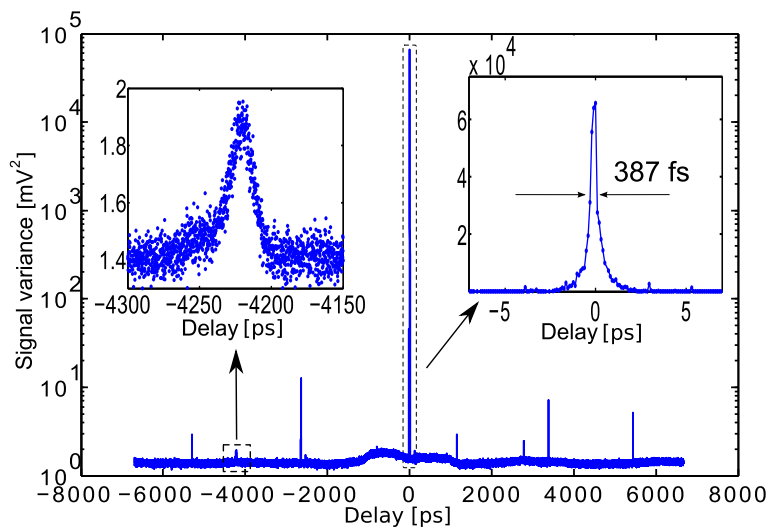

Fig. 4. Semi-logarithmic plot of the variance of the interferometric signal resulting from the averaging of 1.5×10^9 laser shots. The right insert shows a zoom of the main peak evidencing the time resolution (linear scale). The left insert shows a small feature observed 4 ns away from the main peak (linear scale).

The resulting semi-logarithmic plot of the sorted variance signal, shown on Fig. 4, demonstrates the success of the method and the large dynamic range that we could obtain. The data have been sorted according to the time delays in 2^{17} time bins (bin size of 102 fs) and averaged for a total of 1.5×10^9 laser shots, which corresponds to a total acquisition time of 41 s (instead of 16 s if the computer were fast enough to process all laser shots). Note that the delay interval is represented from $-T_1/2$ to $T_1/2$. The main peak, shown in an expanded time scale in the right insert, exhibits a time resolution better than 400 fs FWHM. It is remarkable that a sub-picosecond time resolution is achieved using free running lasers with a simple fiber-based setup. Yet, this value is greater than the width of the time window of 239 fs mentioned above. We first note that the chosen bin size of about 100 fs – four times smaller than the measured value – plays no significant role in the observed broadening, which is thus attributed to two complementary reasons. First, the laser jitter results in uncontrolled fluctuations in the repetition rates between two coincidence events. Second, unlike what we assumed above, there might be a slight imbalance in the amount of spectral phase accumulated in the two 10-m long optical fibers, resulting e.g.

from the combined effect of slightly different initial pulses and some amount of optical non-linearities during the propagation in the fibers. Further work is currently in progress in order to test these hypotheses, consisting e.g. of measuring the time resolution as a function of the time between coincidences since a significant variation would be a signature of the effect of timing jitter.
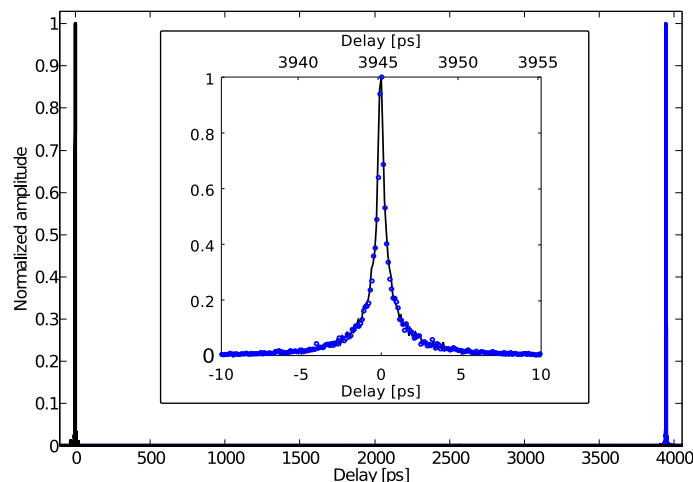

Fig. 5. Linear-scale plot of the variance signal in the same experimental conditions as Fig. 4 (black solid line) and after a delay resulting from free space propagation over a path of about 1.2 m (blue solid line). The insert shows a zoom around the zero time delay (black solid line) and around the delay of 3945 ps (blue circles).

Figure 4 also shows some satellite peaks that we attribute to secondary reflections at various interfaces of the optical setup. For example, the small peak shown in the left insert has a position in time of -4223 ps (modulo T_1) and a duration of 18 ps, calculated by gaussian fit. These values are compatible with the delay and group-velocity dispersion associated with a propagation through 23.6 meters of optical fiber, wich indicates a double passage through a 10-m fiber and the following fiber coupler (1.67 m).

In conventional ASOPS, the time resolution can sometimes deteriorate for large values of the time delay since the corresponding data are acquired far from the coincidence, and are thus more affected by laser timing jitter. Such a behavior is *a priori* not expected in AD-ASOPS since, as will be illustrated with the movie discussed at the end of the article, the time delays occur in a quasi-random fashion instead of the sequential filling encountered in ASOPS. Yet, it is interesting to directly demonstrate that the AD-ASOPS time resolution does not depend on the time delay. For this purpose, we have inserted a free-space propagation of about 1.2 m in one arm of the signal interferometer and measured the corresponding signal, shown in Fig. 5. As expected, we still observe a narrow peak, shifted by a delay of 3945 ps. The insert shows that, apart from the time shift, the signal is exactly identical to that obtained without the free-space propagation, thanks to the negligible dispersion in the additional collimation optics. We thus conclude that our measurement of the time resolution is representative of the whole time range.

As an example of a dynamics over a longer time scale we measured the time response of the photodiode (and acquisition electronics) after its excitation by the pump pulses. This is achieved by replacing the signal part of the above setup with a single photodiode measuring the pump pulses, while the resulting analog signal is measured using the acquisition card clocked at the
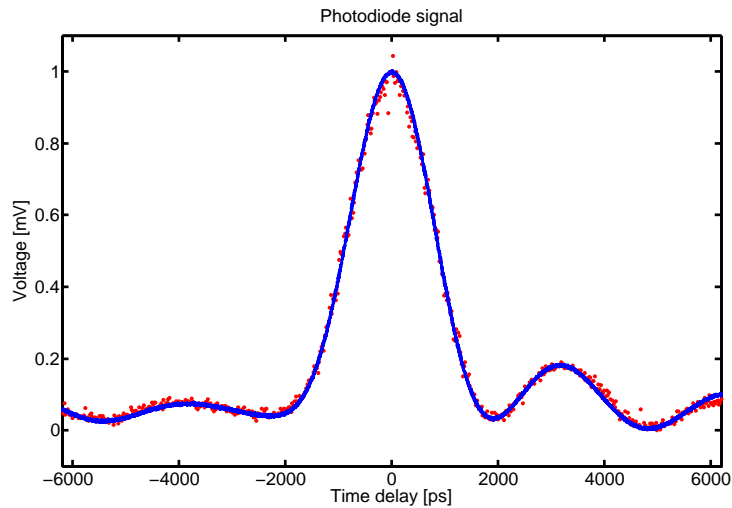
Fig. 6. Time response of the photodiode excited by pump pulses at frequency f_1, acquired with the acquisition card clocked at the probe frequency f_2 and sorted according to the pump-probe delay (blue line). The data are compared with a direct measurement performed with a clock triggered at the pump frequency f_1 while the delay between excitation and acquisition is scanned by purely electronic means (red dots). The figure is the last frame of the associated movie (Media 1) showing the acquisition of the AD-ASOPS data and associated histogram, with an exponentially-accelerating acquisition rate.

probe frequency. As above, the experimental data are sorted according to the pump-probe delay measured with the same coincidence-detection setup. Figure 6 shows the resulting experimental data for 2^{14} time bins (width 816 fs) and a total of 10^6 laser shots. The measured dynamics (blue line), recorded with an acquisition time of only 10.8 ms, is in perfect agreeeent with an alternative measurement (red dots) obtained by a direct measurement of the pump analog signal, repeated for different values of the electronic delay between the pulses and the clock signal of the acquisition card. The associated movie, Fig. 6 (Media 1), shows the progressive build-up of the histogram and signal plots with an exponentially-accelerating acquisition rate. For the first laser shots, the behavior is similar to ASOPS, except that the scanning rate Δf is now considerably greater. The first scan contains only five laser shots and is thus extremely sparse. Note that the delay decreases with time because T_1 is greater than T_2 in our case. The shots associated with the following scans arise at slightly shifted time values so that all time bins are eventually filled. In the last part of the movie, the number of shots per time bin increases, resulting in a steady improvement of the signal to noise ratio.

Note that in the case of this latter experiment, the time resolution is indeed limited by the pump pulse duration at the exit of the optical fiber (~ 11 ps), which is not an issue considering the nanosecond response time of the photodiode and acquisition electronics measured in this case. For pump-probe experiments demanding femtosecond time resolution, it would be preferable to propagate the pump and probe pulses in free space, while keeping the fiber-based setup for coincidence detection.

5. Conclusion

To summarize, we have demonstrated AD-ASOPS, a new approach to asynchronous optical sampling that relies on an *a posteriori* determination of the time delay between pulse pairs, calculated by a linear interpolation of the time delay between coincidences. The method has been shown to have a sub-picosecond time accuracy, which makes it suitable for the rapid acquisition of time-domain data, e.g. for applications in pump-probe spectroscopy, although it is not currently suitable for applications to Fourier-transform spectroscopy - or multi-heterodyne coherent spectroscopy - which require a sub-femtosecond time accuracy. The main advantage of the method is its straightforward implementation on already-existing laser systems, resulting from the fact that there is no requirement on the repetition rates and that its complexity is essentially confined in the electronic apparatus and acquisition software. Moreover, if the two scanning lasers have overlapping spectra, the optical part of the setup can be fiber-based, adding comfort and stability to the setup. In combination with lower repetition-rate laser amplifiers and electronic control of the triggering signal [25, 26], this method could achieve millisecond total delay scan, while conserving the sub-picosecond accuracy.